

# Local compressional and global Alfvén eigenmode structure on NSTX and their effect on core energy transport\*

NA Crocker,<sup>1</sup> E Belova,<sup>2</sup> RB White,<sup>2</sup> ED Fredrickson,<sup>2</sup> NN Gorelenkov,<sup>2</sup> K Tritz,<sup>3</sup> WA Peebles,<sup>1</sup> S Kubota,<sup>1</sup> A Diallo,<sup>2</sup> BP LeBlanc<sup>2</sup> and SA Sabbagh

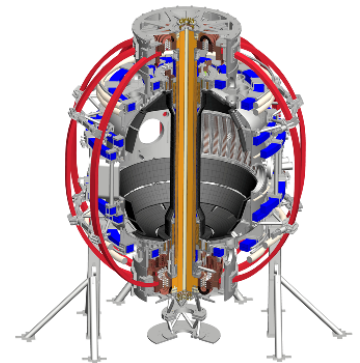
<sup>1</sup>UCLA, <sup>2</sup>PPPL, <sup>3</sup>JHU

NSTX-U/Magnetic Fusion Science Meeting Aug. 27, 2018

\*Supported by US DOE Contracts DESC0011810, DE-FG02-99ER54527 & DEAC0209CH11466

UCLA

PPPL



# Novel reflectometry analysis improves CAE & GAE measurements and understanding of $\chi_e$

- Motivation – compressional (CAE) and Global Alfvén eigenmodes (GAE) proposed to cause high anomalous core  $\chi_e$
- New multi-channel reflectometer analysis  $\Rightarrow$  more accurate  $\delta n$  amplitude and structure
- $\delta n$  used to test hypothesis for anomalous core  $\chi_e$ 
  - simulation of  $e^-$  drift orbit modification predicts  $\chi_e$  – compared to TRANSP
- $\delta n$  compared to HYM simulations
- $\delta n$  used with HYM to test alternate hypothesis – CAE-KAW coupling

# Motivation: CAEs & GAEs candidates for core energy transport in NSTX

- CAEs & GAEs excited by Doppler-shifted cyclotron resonance with beam ions

[N. N. Gorelenkov, NF 2003]

- CAE & GAE activity correlates with enhanced  $\chi_e$  in core

[D. Stutman, PRL 2009; K. Tritz, APS 2010 Invited Talk; N. A. Crocker, PPCF 2011]

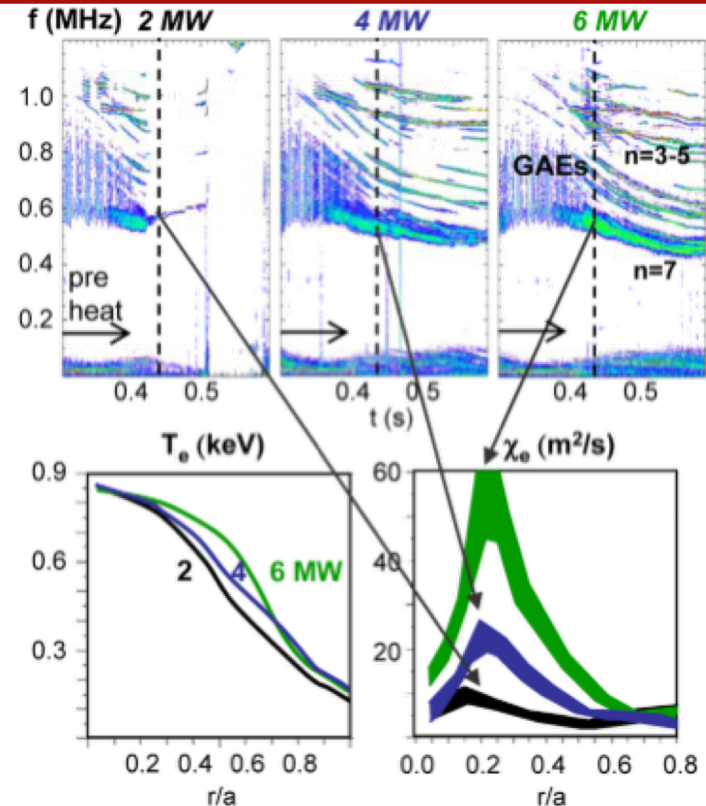
- $T_e$  profile flattens as  $P_{NB}$  increases

- $\chi_e$  from TRANSP modeling

- Two leading hypotheses:

- Stochastization of  $e^-$  guiding center orbits enhance  $\chi_e$  [NN Gorelenkov, NF 2010]

- Coupling to KAWs = missing transport channel  $\Rightarrow$  TRANSP gets  $\chi_e$  wrong [Ya.I. Kolesnichenko, PRL 2010, E.V. Belova, PRL 2015]



[D. Stutman et al., PRL 102 115002 (2009)]

# Reflectometer array measures $\delta n$ of CAEs & GAEs

- Reflectometer array sees global modes identified as CAEs & GAEs

[N.A. Crocker, PPCF 2011]

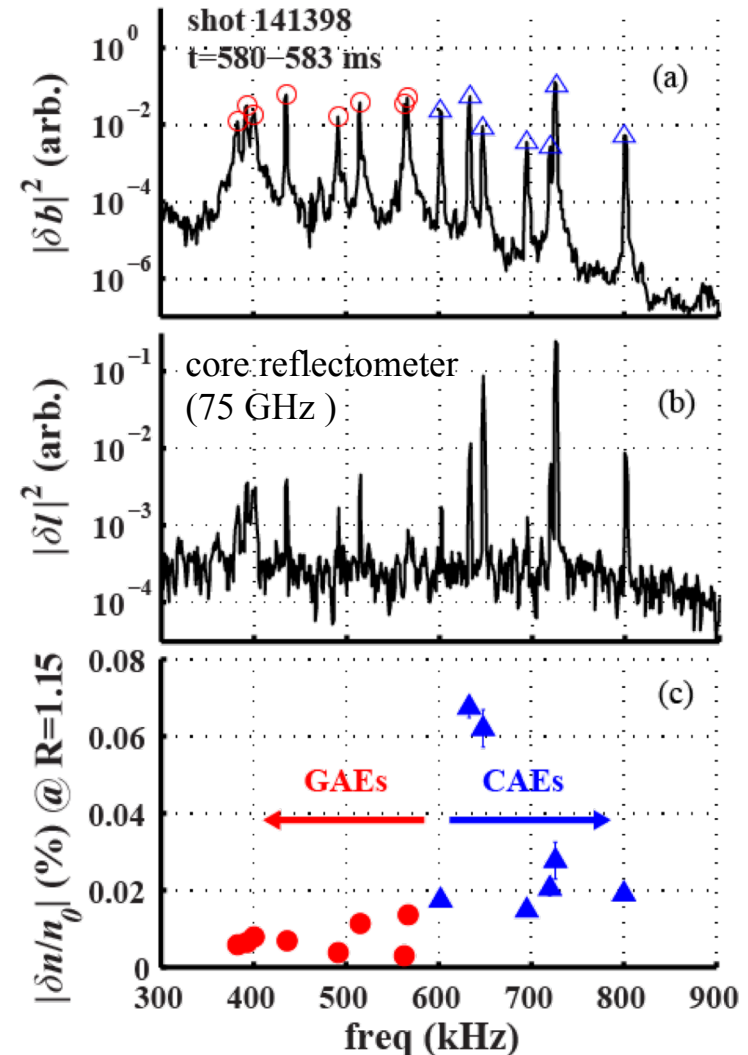
- New analysis gives  $\delta n/n_0$  in core:

– CAE:  $\delta n/n_0 \sim 10^{-4} - 10^{-3}$

– GAE:  $\delta n/n_0 \sim 10^{-5} - 10^{-4}$

- $\delta n$  from measurements via “synthetic diagnostic”

- Reflectometer “signal-to-noise” improved via correlation with  $\delta b$

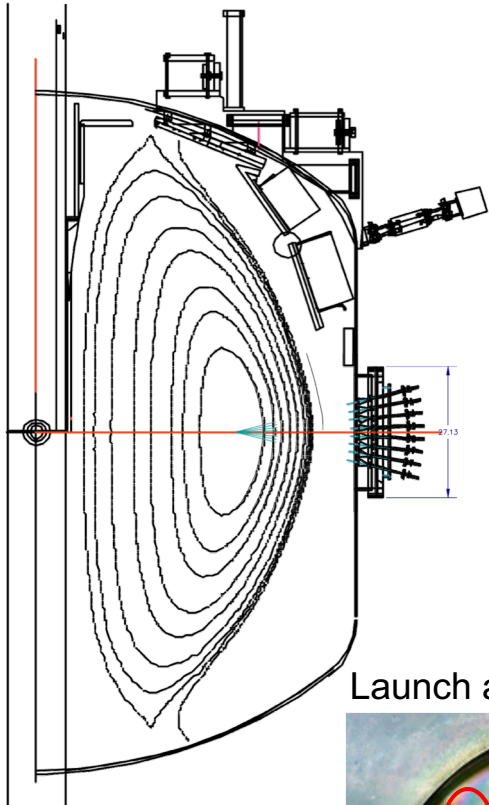




# Measurement Technique

# Reflectometers provide radial array of measurements

NSTX cross-section

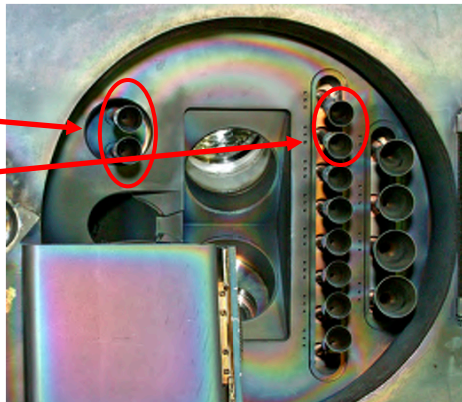


- 16 channels in two arrays: “Q-band” & “V-band”  
– 30 – 50 GHz & 55 – 75 GHz
- Arrays closely spaced  
– Separate launch/receive horn pair for each array
- Propagation direction:  $-\hat{R} \Rightarrow$   
frequency array = radial array
- large radial range in high  $n_e$  plasmas  
( $n_0 \sim 1 - 7 \times 10^{19} \text{ m}^{-3}$ )

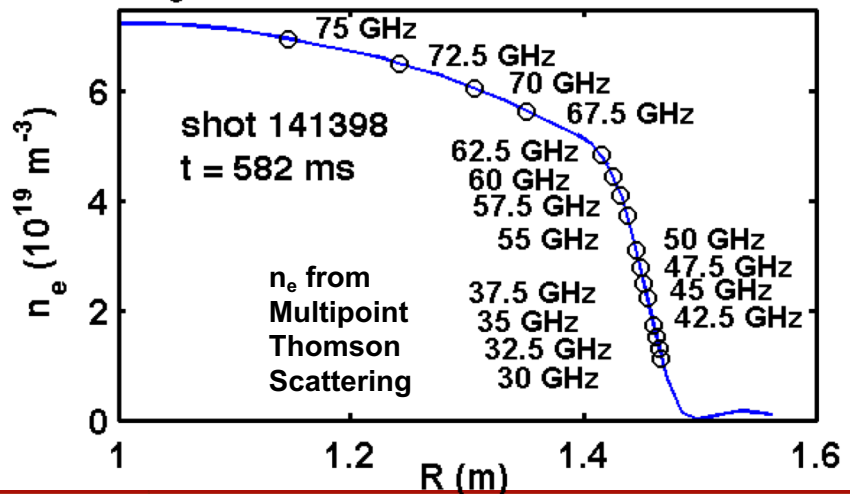
Launch and Receive Horns

30-50 GHz

55-75 GHz

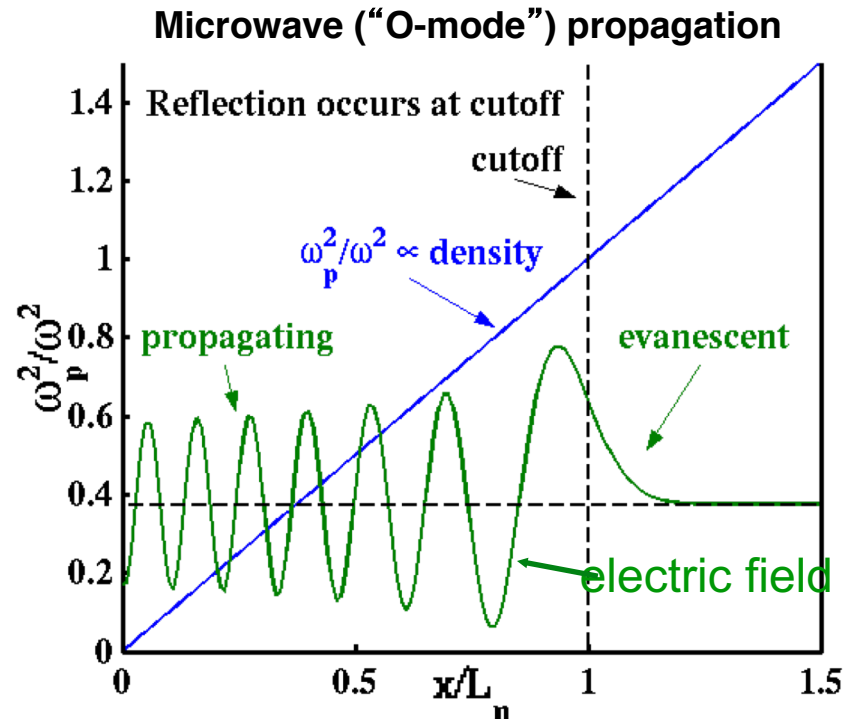


$n_e$  and O-mode cutoff locations



# Reflectometers measure density fluctuations in plasma

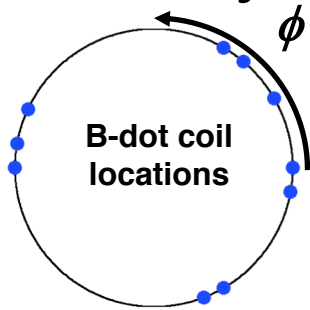
- Microwaves reflect at “cutoff”
  - O-mode:  $\omega^2 = \omega_p^2 + c^2 k^2$
  - microwaves reflect at  $k = 0$  ( $\omega_p = \omega$ )
- Measurement: path length fluctuations ( $\delta l$ ) caused by  $\delta n$



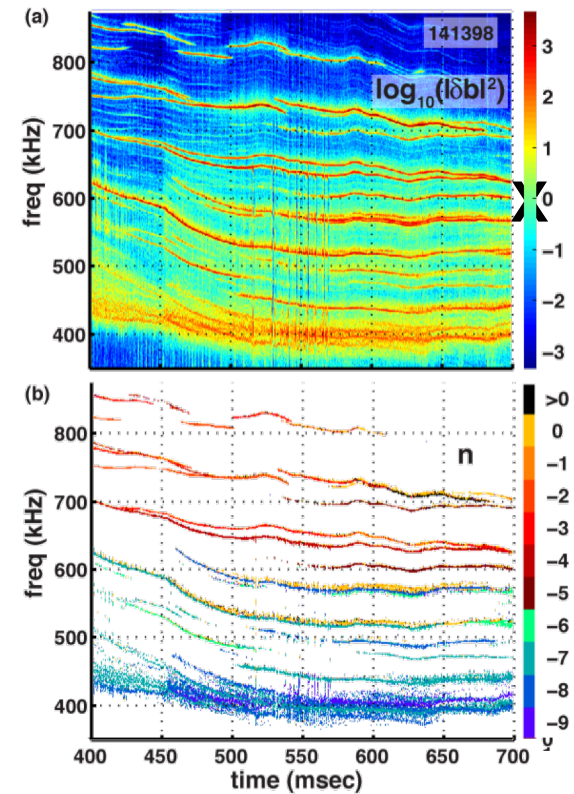
- $\delta l$  sensitive to cutoff motion, but  $\delta n$  along path contributes (a.k.a. “interferometer effect”)
  - cutoff motion dominates as  $k_r \rightarrow 0$  (rigid displacement)

# Toroidal mode numbers and frequencies determined with edge B-dot array

- Modes appear as peaks in  $\delta b$  spectrum
- $n$  determined from  $\delta b$  measured by edge toroidal array of B-dot coils



- Smallest coil spacing is  $10^\circ \Rightarrow$  can distinguish  $|n| \leq 18$



N. A. Crocker, et al. Nucl. Fusion 2013

# Reflectometer Analysis Technique



# $\delta n$ determined via synthetic diagnostic

- Synthetic diagnostic models path length
  - WKB path length integral:

$$l = l_0 + \delta l = \int_{R_{edge}}^{R_{cutoff}} dR \sqrt{1 - \omega_p^2(R)/\omega^2}$$

$$\omega_p^2(R_{cutoff}) = \omega^2, \omega_p^2 = \omega_{p0}^2 + \delta\omega_p^2 \propto n_0 + \delta n$$

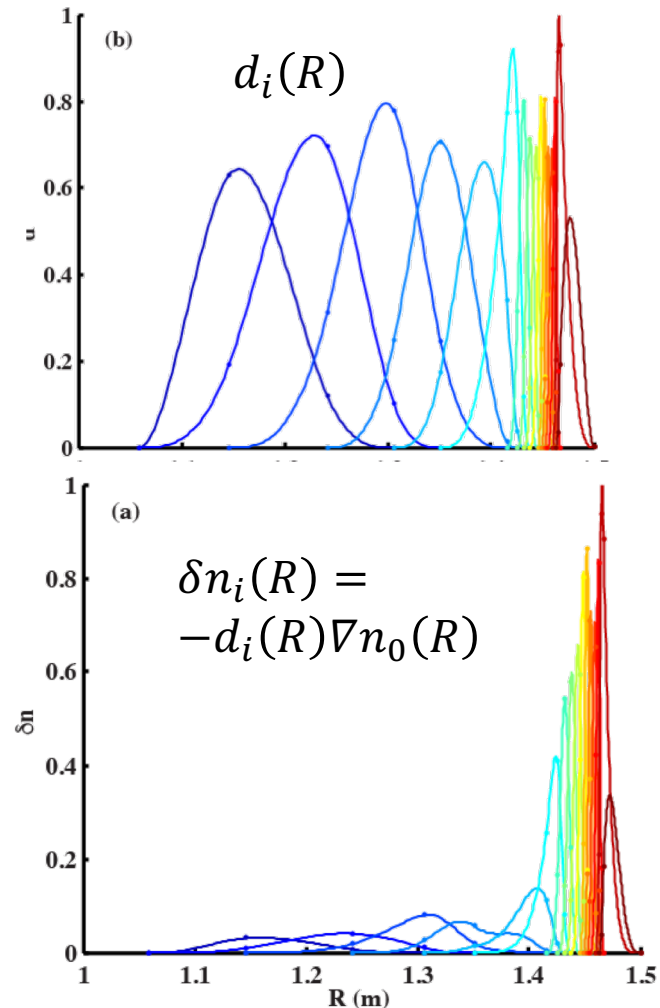
- $\delta n$  modeled with cutoff displacement (d) basis functions:

$$\delta n(R) = -\nabla n_0(R) \sum_i a_i d_i(R)$$

- cubic B-splines for  $d_i(R)$
- set of  $a_i \Rightarrow \delta l_{fit}$  for all channels
- find of set of  $a_i$  to minimize

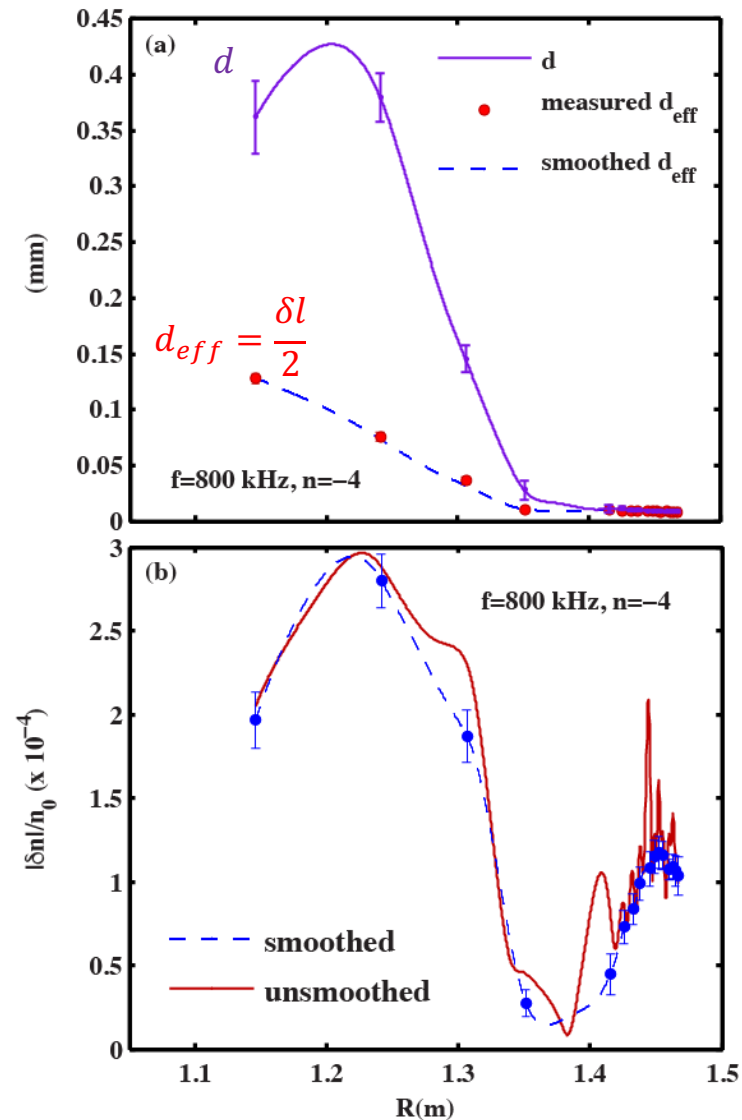
$$\chi^2 = \sum_j (\delta l_{j,meas} - \delta l_{j,fit})^2 / (\sigma_{j,meas}^2)$$

Cutoff displacement basis functions (cubic “B-splines”; cutoff locations as knots)

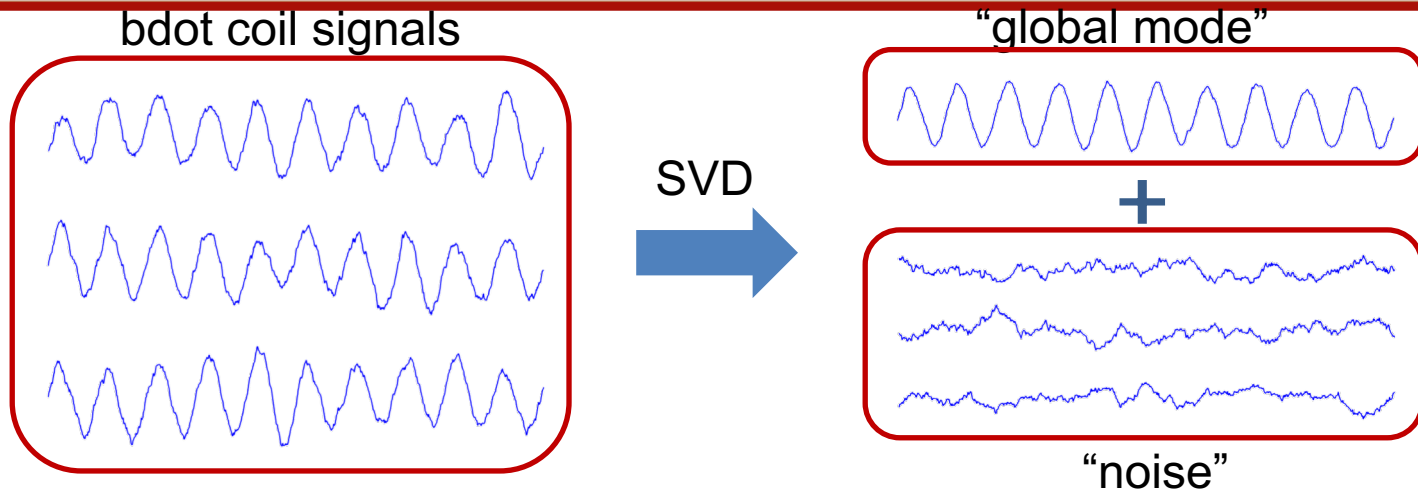


# $\delta n$ determined via synthetic diagnostic

- Fit naturally yields  $d(R)$  along with  $\delta n(R)$
- Fit sensitive to noise  
 $\Rightarrow$  *use smoothed  $\delta l_{meas}$  for inversion*
  - smoothing = low spatial filter
  - smoothed  $\delta l$  within uncertainty of  $\delta l_{meas}$
  - can't know if short scale structure in  $\delta n$  is real, given uncertainties



# Singular value decomposition gives better “global mode” $\delta b$



- global mode observed by 10 bdot coils (HN array)
- “filter” signals with SVD  $\Rightarrow$  global mode w/reduced noise
  - SVD factors space & time dependence of signal matrix:

$$b_{jk} = \tilde{b}_j(t_k) \rightarrow \tilde{b}_{0j} \tilde{b}_{global}(t_k) + \epsilon_j(t_k)$$

- Steps *before* SVD ...

1) bandpass filter coil signals to isolate mode

2) make signals complex  $\Rightarrow$  spatial phase (e.g.  $n\phi_j$ ) factors out automatically:

$$\tilde{b}_j(t) = A(t) \cos(\theta(t) + \theta_{0j}) \rightarrow \hat{\tilde{b}}_j(t) = \frac{1}{\sqrt{2}} A(t) e^{i((\theta(t) + \theta_{0j}))} = \frac{1}{\sqrt{2}} \int_0^\infty d\omega e^{i\omega t} \int_{-\infty}^\infty dt' \tilde{b}(t') e^{-i\omega t'}$$

# SVD finds global mode from eigenvector of signal correlation matrix

- SVD solves factoring problem

$$\hat{b}_j(t_k) = \hat{b}_{0j} \hat{b}_{global}(t_k) + \hat{\epsilon}_j(t_k)$$

- by minimizing  $\chi^2$ :

$$\chi^2 = \sum_{j,k} \left| \hat{b}_j(t_k) - \hat{b}_{0j} \hat{b}_{global}(t_k) \right|^2$$

- $\Rightarrow$  spatial coefficients ( $\hat{b}_{0j}$ ) of global mode from **eigenvector** of correlation matrix **with largest eigenvalue**:

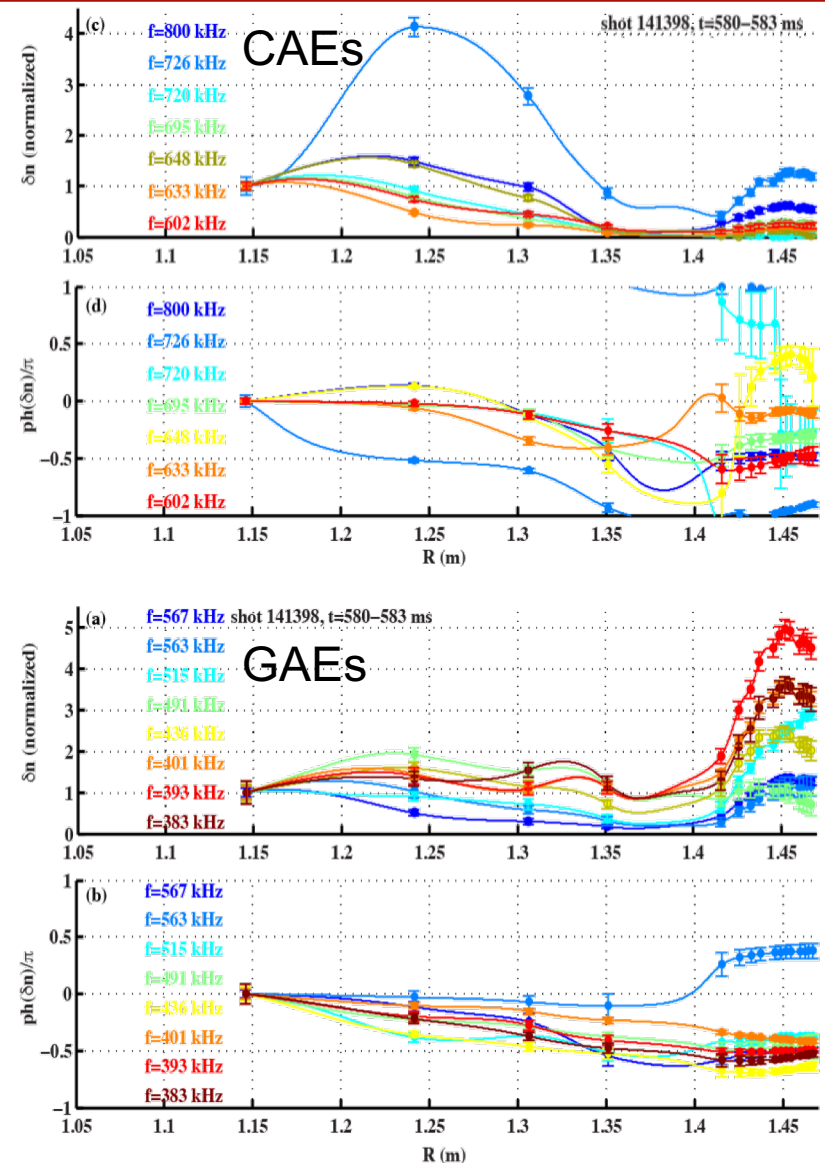
$$\mathbf{C} \hat{\mathbf{b}}_0 = \lambda \hat{\mathbf{b}}_0$$
$$[\mathbf{C}]_{ij} = \left\langle \hat{b}_i(t) \hat{b}_j^*(t) \right\rangle, [\hat{\mathbf{b}}_0]_j = \hat{b}_{0j}$$

# Results of Reflectometer Analysis



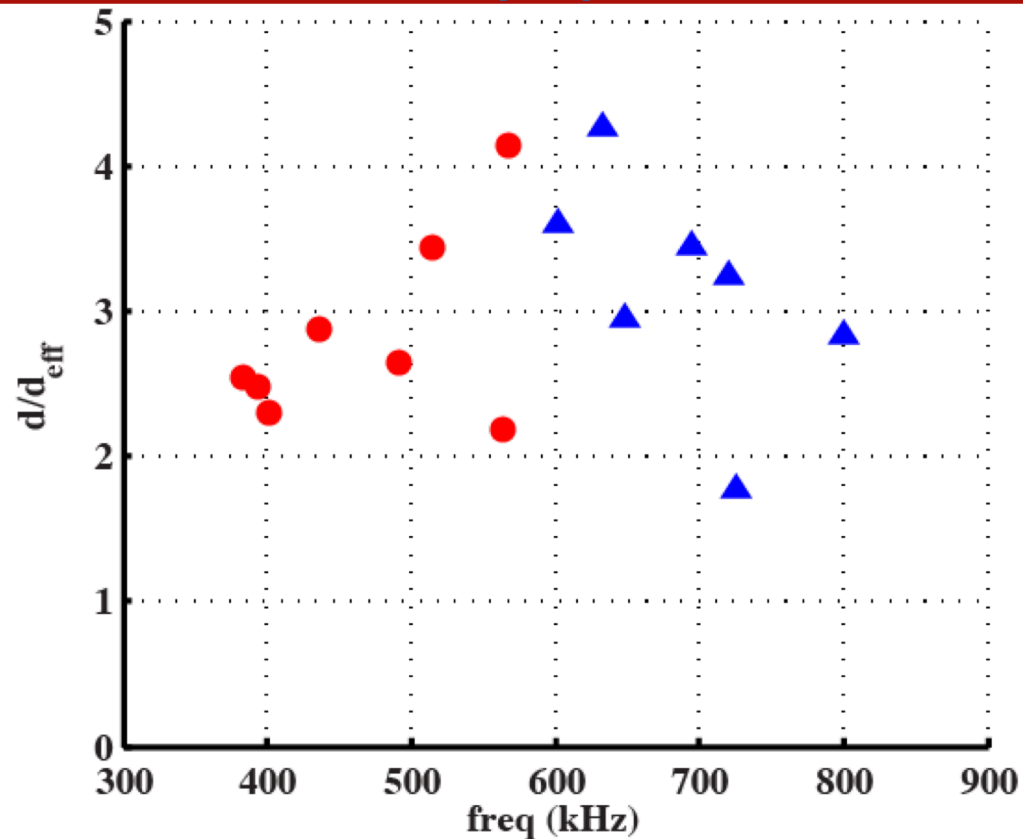
# CAEs and GAEs have different $\delta n$ structure

- CAEs have large, broad core peaks & small edge amplitude
- GAEs have low amplitude, broad structure in core & large edge peaks
- Note: large edge peaks can be caused by small edge radial displacements



# New analysis gives 2–4 x larger cutoff displacement ( $d$ )

- Old analysis:  
 $d_{eff} = \delta l / 2$ 
  - $\delta l$  attributed to cutoff displacement (“mirror approximation”)
- New  $d$  is 2 – 4 x larger  
 $\Rightarrow$  larger plasma displacement



- **Cutoff displacement  $\neq$  plasma displacement**
  - Compression also causes cutoff displacement

# Plasma displacement ( $\xi$ ) estimated from $\delta n$

- Get  $\xi$  from measurement:

$$\delta n/n_0 = -\nabla \cdot \xi - \xi \cdot \nabla \ln(n_0)$$

- Neglect finite  $\omega/\omega_{ci}$ ,  
assume  $E_{\parallel} = 0$

$$\nabla \cdot \xi = \nabla \cdot ((\mathbf{E} \times \mathbf{B}) / (-i\omega B^2))$$

$$\approx -\delta b_{\parallel} / B_0 - \xi \cdot \left( \frac{1}{2} \beta \nabla \ln(p_0) + 2 \nabla \ln(B_0) \right)$$

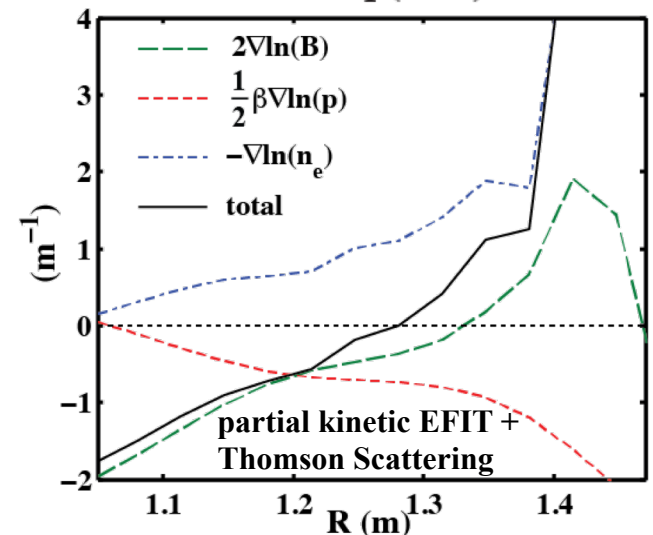
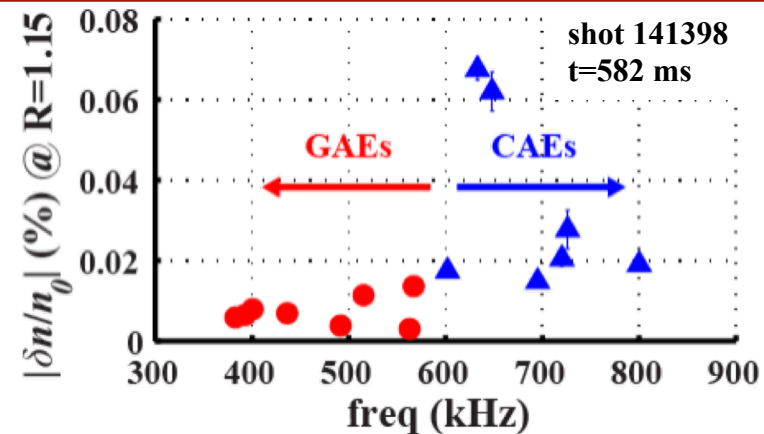
- GAEs:  $\xi_R \approx 0.7 L_n \delta n/n$   
@  $R = 1.15$  m

– assume  $\tilde{b}_{\parallel} = 0$

–  $L_n \sim 1.7$  m

–  $n_0/n \approx 1.05$

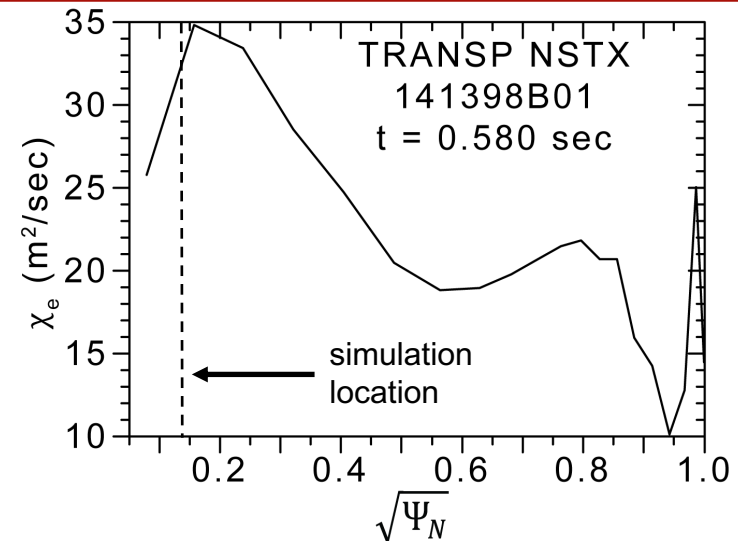
- CAEs:  $\delta n/n_0 \approx -\nabla \cdot \xi \approx \delta b_{\parallel} / B_0$



# Prediction of $\chi_e$ and comparison with TRANSP

# $\chi_e$ from GAEs simulated for 6 MW H-mode 141398, t = 0.58 sec

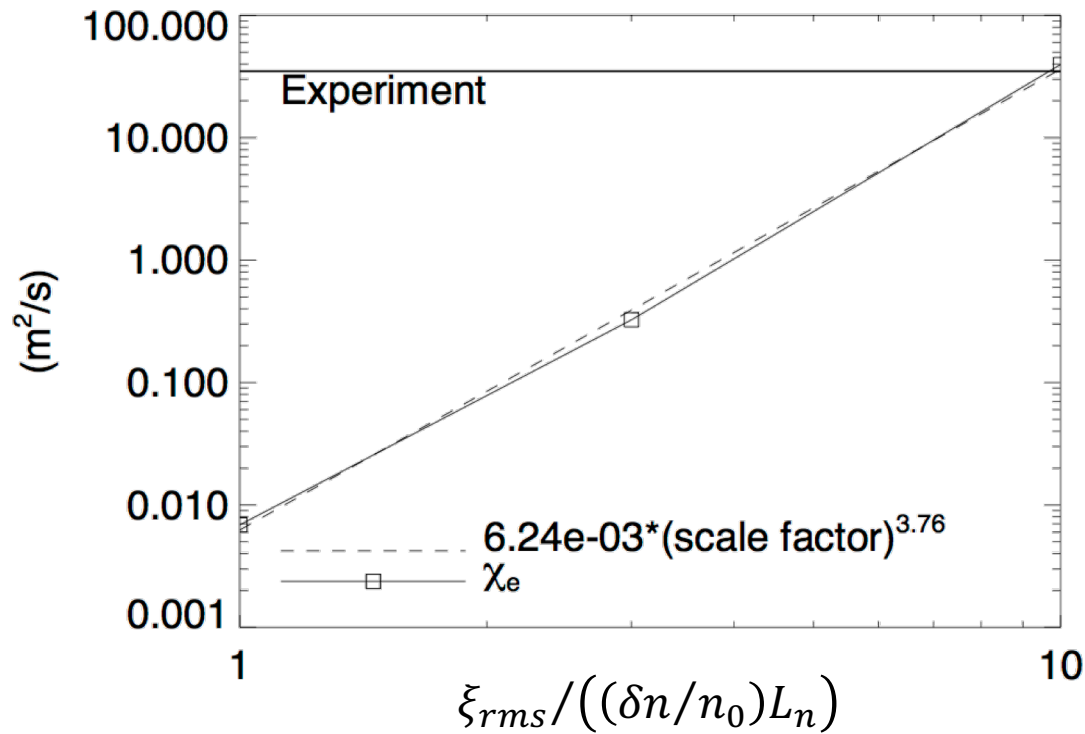
- Anomalous core  $\chi_e$  ( $\sim 35$  m<sup>2</sup>/s) in 6 MW H-mode
- $e^-$  guiding center orbit spreading simulated by ORBIT  $\Rightarrow \chi_e$  (see e.g. [NN Gorelenkov NF 2010])
  - B-field from experiment ( $B_{T0}=0.45$  T)
  - at  $t = 0$ , isotropic thermal population ( $T_e = 1$  keV),  $\delta$ -function at  $\Psi_N^{1/2} = 0.15$
  - collisionless
  - population spreads with time  $\Rightarrow D_e, \chi_e = \frac{3}{2}D_e$
- 8 GAEs
  - $\xi_{rms} \sim 0.4$  mm (using  $\xi \approx (\delta n/n_0)L_n$ )
  - $\omega = k_{\parallel} V_A \Rightarrow |m| = 0 - 2$
  - poloidal+toroidal Fourier modes used



| $f$ (kHz) | $n$ | $m$ | $\xi$ (mm) |
|-----------|-----|-----|------------|
| 383       | -8  | -2  | 0.1        |
| 393       | -7  | -1  | 0.11       |
| 401       | -8  | -2  | 0.13       |
| 436       | -7  | 0   | 0.12       |
| 491       | -8  | 0   | 0.06       |
| 515       | -7  | 1   | 0.21       |
| 563       | -6  | 2   | 0.05       |
| 567       | -8  | 1   | 0.25       |



# $\chi_e$ from GAEs in simulation much less than from TRANSP



- $\chi_e \ll 1 \text{ m}^2/\text{s}$  for  $\xi_{rms} \sim (\delta n/n_0)L_n$
- scaling study  $\Rightarrow \chi_e$  sensitive to amplitude ( $\chi_e \propto \xi^{3.76}$ )
- need  $\xi = 10 * \xi_{rms}$  for agreement with TRANSP

# Inclusion of CAEs as shear modes increases simulated $\chi_e$ , but still not enough

- 7 CAEs (15 modes total)
- If CAEs are shear modes:  
 $\text{CAE } \delta n \gg \text{GAE } \delta n \Rightarrow \text{CAE } \xi \gg \text{GAE } \xi$ 
  - $\xi_{rms} \sim 1.8$  mm for CAEs (1.9 mm all modes)
  - using  $\xi \approx (\delta n/n_0)L_n$
- Shear CAEs  $\Rightarrow$  large  $m$ 
  - $\omega = k_{||} V_A \Rightarrow |m| = 4-10$
- $\chi_e = 8$  m<sup>2</sup>/s at  $\xi_{rms} \sim 1.9$  mm
  - expect 2 m<sup>2</sup>/s from GAE-only simulation scaling
    - more modes = more stochastic?
- Need  $\xi_{rms} \sim 3*(1.9$  mm) for  $\chi_e = 34$  m<sup>2</sup>/s  $\sim \chi_{e, \text{expt}}$

| $f$ (kHz) | $n$ | $m$ | $\xi$ (mm) |
|-----------|-----|-----|------------|
| 602       | -5  | 4   | 0.31       |
| 633       | -4  | 5   | 1.23       |
| 648       | -1  | 8   | 1.05       |
| 695       | -5  | 5   | 0.26       |
| 720       | 0   | 10  | 0.36       |
| 726       | -3  | 7   | 0.57       |
| 800       | -4  | 7   | 0.32       |

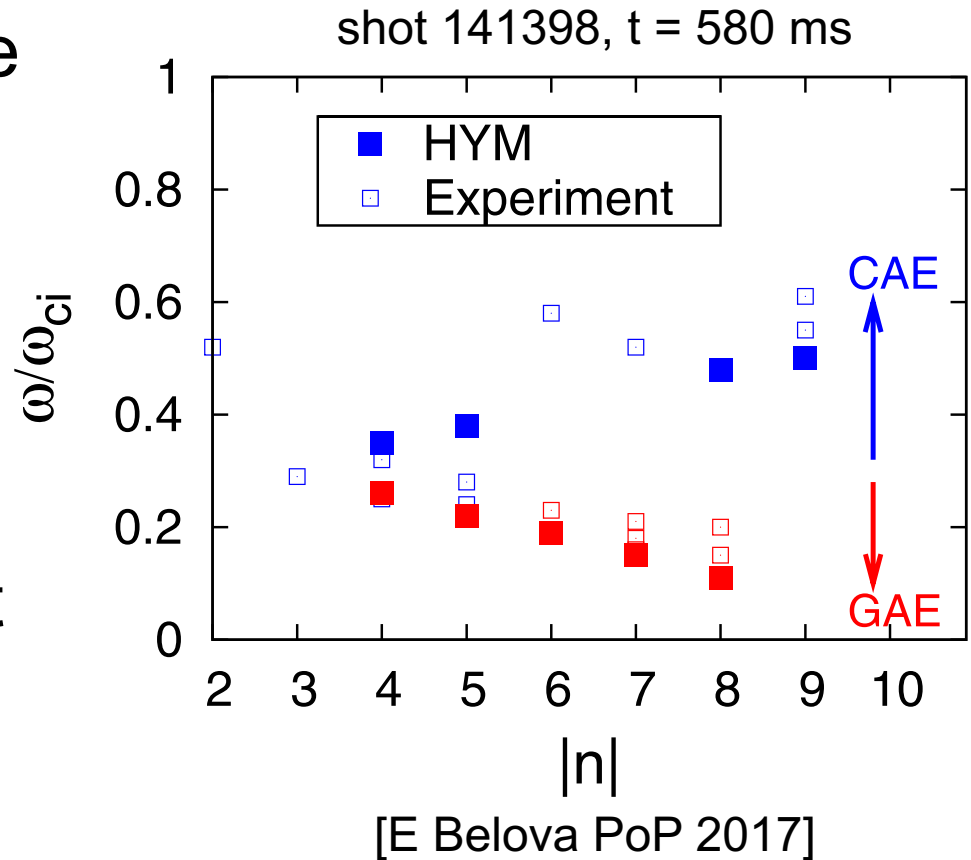
# Comparison with HYM Simulation and Test of CAE-KAW Coupling

# Initial comparison of HYM simulation & measurement promising

- Hybrid MHD (HYM) code simulates CAE structure & stability

- 3D, ideal MHD fluid &  $\delta f$  solver full orbit fast-ions
- realistic equilibrium

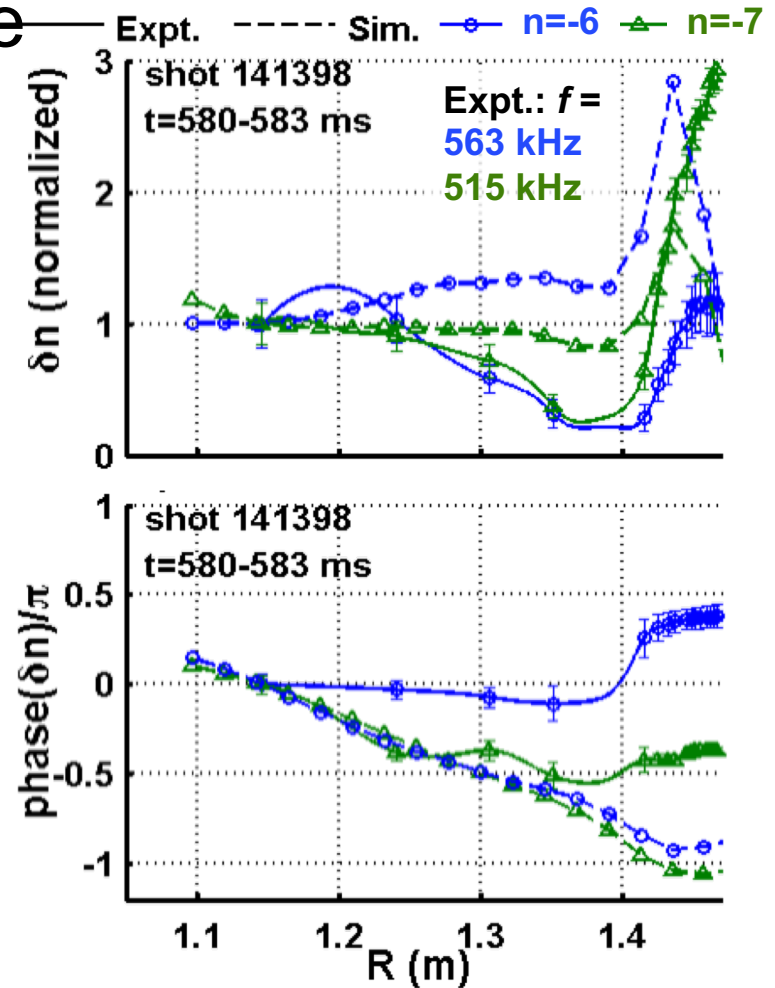
- Simulation & experiment compared for beam heated H-mode plasma



- Most-unstable modes have  $f$  &  $n$  similar to observed experimental spectrum [E Belova PoP 2017]

# Initial comparison of HYM simulation & measurement promising

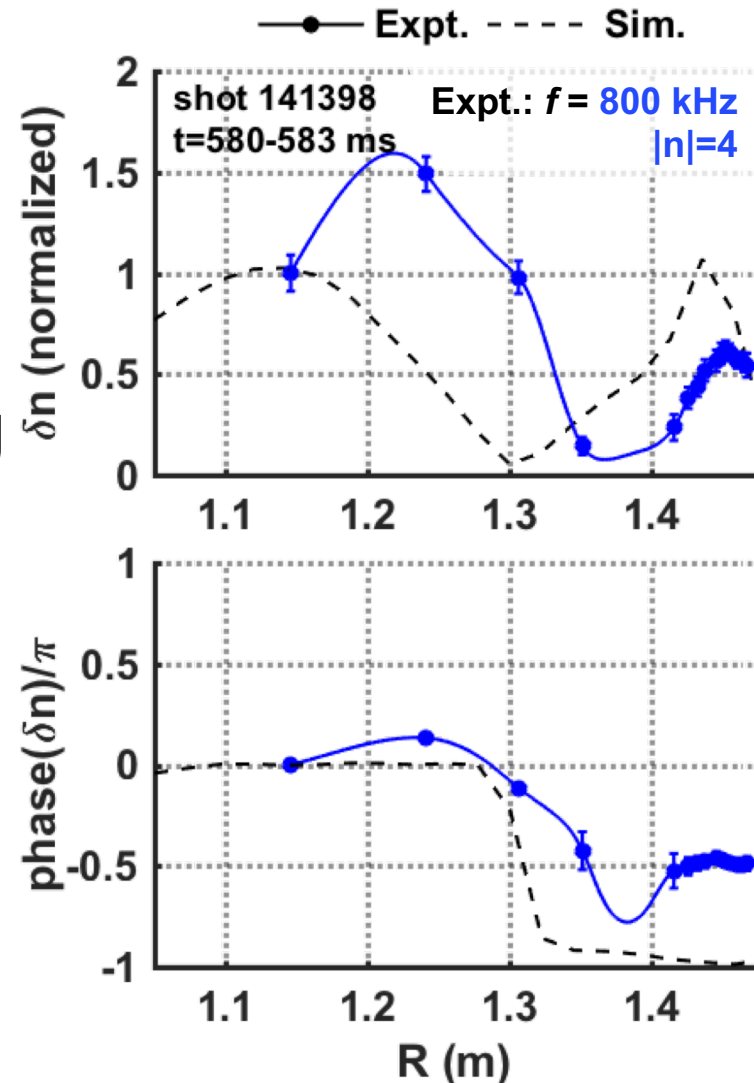
- HYM simulation: most unstable  $n = 6$  & 7 modes counter propagating GAEs
- Structure similarities: broad core & strong edge peaking
- Simulation shows stronger phase change across minor radius
- Expect structure sensitive to
  - $B_0$  structure – included in HYM
  - Hall effect (finite  $\omega/\omega_{ci}$ ) & toroidal rotation – under development for HYM





# Initial comparison of HYM simulation & measurement promising

- CAE structure similarities: broad core peaks & small edge amplitude
- CAEs co-propagating in simulation; counter-propagating in experiment.
  - further work needed to understand
- Expect structure sensitive to
  - $|B_0|$  structure – included in HYM
  - Hall effect (finite  $\omega/\omega_{ci}$ ) & toroidal rotation – under development for HYM



# Measurements + Simulation $\Rightarrow$ Small CAE-KAW energy transport

- HYM:  $n = 4$  CAE,  $\frac{\delta b_{\parallel}}{B_0} \sim 6.6 \times 10^{-3} \Rightarrow P = 1.2 \text{ MW}$

CAE-KAW energy coupling transport: [E Belova PoP 2017]

– simulation  $\xi$  scaled to  $d_{eff} \Rightarrow \frac{\delta b_{\parallel}}{B_0} \sim 0.9 - 3.4 \times 10^{-3}$

- New approach:  $\delta n/n \approx \delta b_{\parallel}/B$  in core  $\Rightarrow$   
 $2 \times 10^{-4} < \delta b_{\parallel}/B < 7 \times 10^{-4}$

–  $\delta n/n_0$  measured @  $R=1.15 \text{ m}$

- $P \propto \delta b_{\parallel}^2 \Rightarrow P = 0.03 \text{ MW}$  total for all modes

– assume  $P/\delta b_{\parallel}^2$  same for all modes

- Could improve estimate by rescaling HYM modes with measured  $\delta n/n$ .

# Conclusions and Future Work

# New $\delta n$ measurements advance understanding of CAE & GAE effect on core energy transport

- New multi-channel reflectometer analysis  $\Rightarrow$  more accurate  $\delta n$  internal amplitude and structure
  - cutoff displacement larger than previous analysis
- GAE modification of  $e^-$  drift orbits  $\Rightarrow$  GAEs (or GAE+shear CAEs) too small to explain  $\chi_e$  from TRANSP
- Measured and simulated GAE structures show rough similarities
  - HYM development currently under way may explain differences
- New  $\delta n$  + HYM Poynting Flux  $\Rightarrow$  CAE-KAW energy flux small

# Many avenues for future work

- Improve reflectometer analysis
  - better synthetic diagnostic  $\Rightarrow$  raytracing
  - better alternatives to SVD filtering?
- Improve ORBIT modeling
  - better GAEs (finite  $\omega/\omega_{ci}$ , realistic poloidal structure,...)
  - ORBIT modified for CAEs. Requires verification...
  - simulation with modes from HYM (or other codes)
  - better electromagnetic amplitudes from  $\delta n$

# Many avenues for future work

- Understand simulation & measured structure differences
  - exploit measured phase to understand role of Hall effect & rotation?
- Improve CAE-KAW estimate from HYM: rescale HYM modes with measured  $\delta n/n$

# Appendix: Plasma displacement ( $\xi$ ) estimated from $\delta n$

- Get  $\xi$  from measurement:  $\delta n/n_0 = -\nabla \cdot \xi - \xi \cdot \nabla \ln(n_0)$
- Neglect finite  $\omega/\omega_{ci}$ , Assume  $E_{\parallel} = 0$  &  $\mathbf{J}_0 \times \mathbf{B}_0 - \nabla p_0 = 0$

$$\begin{aligned}
 \nabla \cdot \xi &= \nabla \cdot \left( \frac{\delta \mathbf{E} \times \mathbf{B}_0}{-i\omega B_0^2} \right) = \frac{\mathbf{B}_0}{-i\omega B_0^2} \cdot \nabla \times \delta \mathbf{E} - \frac{\delta \mathbf{E}}{-i\omega} \cdot \nabla \times \frac{\mathbf{B}_0}{B_0^2} \\
 &= \frac{\mathbf{B}_0}{-i\omega B_0^2} \cdot \nabla \times \delta \mathbf{E} - \frac{\delta \mathbf{E}}{-i\omega B_0^2} \cdot \nabla \times \mathbf{B}_0 - \frac{\delta \mathbf{E}}{-i\omega} \cdot (\nabla B_0^{-2} \times \mathbf{B}_0) \\
 &= -\frac{\delta \mathbf{B} \cdot \mathbf{B}_0}{B_0^2} - \frac{\mu_0 \delta \mathbf{E}}{-i\omega B_0^2} \cdot \mathbf{J}_0 + \frac{2\delta \mathbf{E}}{-i\omega B_0^2} \cdot (\nabla \ln(B_0) \times \mathbf{B}_0) \\
 &= -\frac{\delta \mathbf{B} \cdot \mathbf{B}_0}{B_0^2} - \mu_0 \frac{\delta \mathbf{E} \times \mathbf{B}_0}{-i\omega B_0^4} \cdot \nabla p_0 - \frac{2\delta \mathbf{E} \times \mathbf{B}_0}{-i\omega B_0^2} \cdot \nabla \ln(B_0) \\
 &= -\frac{\delta \mathbf{B} \cdot \mathbf{B}_0}{B_0^2} - \frac{1}{2} \beta \xi \cdot \nabla \ln(p_0) - 2\xi \cdot \nabla \ln(B_0)
 \end{aligned}$$